

See discussions, stats, and author profiles for this publication at: <https://www.researchgate.net/publication/259565874>

Theoretical Kinetics Study of the F(P-2) + NH₃ Hydrogen Abstraction Reaction

ARTICLE in THE JOURNAL OF PHYSICAL CHEMISTRY A · JANUARY 2014

Impact Factor: 2.69 · DOI: 10.1021/jp4118453 · Source: PubMed

CITATIONS

9

READS

48

4 AUTHORS:



Joaquin Espinosa-Garcia

Universidad de Extremadura

141 PUBLICATIONS 2,187 CITATIONS

SEE PROFILE



Antonio Fernández-Ramos

University of Santiago de Compostela

84 PUBLICATIONS 1,832 CITATIONS

SEE PROFILE



Yury Suleimanov

The Cyprus Institute

38 PUBLICATIONS 404 CITATIONS

SEE PROFILE



Jose C Corchado

Universidad de Extremadura

118 PUBLICATIONS 3,297 CITATIONS

SEE PROFILE

Theoretical Kinetics Study of the $F(^2P) + NH_3$ Hydrogen Abstraction Reaction

J. Espinosa-Garcia,^{*,†} A. Fernandez-Ramos,[‡] Y. V. Suleimanov,^{§,||} and J. C. Corchado[†]

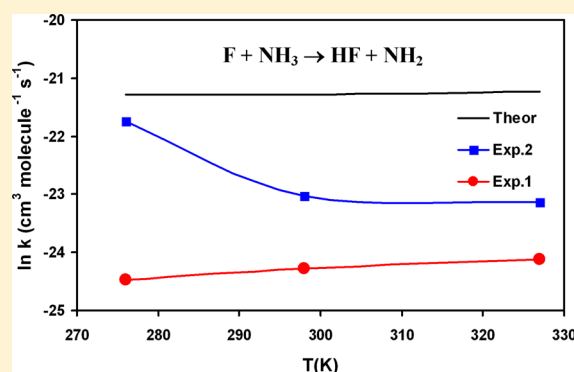
[†]Departamento de Química Física, Universidad de Extremadura, 06071 Badajoz, Spain

[‡]Departamento de Química Física y Centro Singular de Investigación en Química Biológica y Materiales Moleculares (CIQUS), Universidad de Santiago de Compostela, 15782 Santiago de Compostela, Spain

[§]Department of Chemical Engineering, Massachusetts Institute of Technology, 77 Massachusetts Avenue, Cambridge, Massachusetts 02139, United States

^{||}Department of Mechanical and Aerospace Engineering, Combustion Energy Frontier Research Center, Princeton University, Olden Street, Princeton, New Jersey 08544, United States

ABSTRACT: The hydrogen abstraction reaction of fluorine with ammonia represents a true chemical challenge because it is very fast, is followed by secondary abstraction reactions, which are also extremely fast, and presents an experimental/theoretical controversy about rate coefficients. Using a previously developed full-dimensional analytical potential energy surface, we found that the $F + NH_3 \rightarrow HF + NH_2$ system is a barrierless reaction with intermediate complexes in the entry and exit channels. In order to understand the reactivity of the title reaction, thermal rate coefficients were calculated using two approaches: ring polymer molecular dynamics and quasi-classical trajectory calculations, and these were compared with available experimental data for the common temperature range 276–327 K. The theoretical results obtained show behavior practically independent of temperature, reproducing Walther–Wagner’s experiment, but in contrast with Persky’s more recent experiment. However, quantitatively, our results are 1 order of magnitude larger than those of Walther–Wagner and reasonably agree with the Persky at the lowest temperature, questioning so Walther–Wagner’s older data. At present, the reason for this discrepancy is not clear, although we point out some possible reasons in the light of current theoretical calculations.



1. INTRODUCTION

The $F + NH_3$ reaction is difficult to study experimentally because it is very fast, followed by extremely fast secondary atom/radical reactions, $F + NH_2 \rightarrow HF + NH$. It is also difficult to study theoretically because the accurate description of low-energy barriers requires a very high level of quantum chemistry theory.

The title reaction has been studied theoretically in the past a few times,^{1–6} although recently there has been renewed interest in this reaction.^{4–6} These theoretical studies contrast with the extensive experimental literature,^{1,4,7–18} both kinetics and dynamics. From the dynamics point of view, Sloan et al.^{1,12,14} and Wategaonkar and Setser¹³ reported an inverted vibrational distribution of the HF product. These authors found theoretically a hydrogen-bonded $FH \cdots NH_2$ complex in the exit channel, which causes a randomization of the reaction exoergicity among all available product degrees of freedom. In addition, Goddard et al.¹ also found this complex theoretically using high-level ab initio calculations with energy 8.1 kcal mol^{–1} lower than the products. More recently, Misochko et al.^{16,17} in their infrared and EPR spectroscopic studies observed for the first time this intermediate complex, $FH \cdots NH_2$. From the

kinetics point of view, there is a controversy about the positive/negative activation energy for the forward reaction. Thus, while the experiment of Walther and Wagner¹⁸ reported conventional temperature dependence, and consequently positive activation energy, Persky’s more recent experiment¹⁵ in the temperature range 276–327 K reported inverse temperature dependence, and these values are 1 order of magnitude larger. To explain this behavior, Persky suggested the existence of an intermediate complex in the entry channel. Therefore, intermediate complexes in the entry and exit channels may affect the reaction kinetics and dynamics, and whether they have an influence becomes an important issue.

Recently, Xiao et al.⁴ and Feng et al.⁵ using very high-level ab initio calculations investigated some complexes in the entry and exit channels for the title reaction. However, the multiple electronic states due to the open-shell character of the system were not taken into account.

Received: December 3, 2013

Revised: January 2, 2014

Published: January 2, 2014

Finally, in 2011 some of us⁶ performed a dynamics study on the title reaction using quasi-classical trajectory (QCT) calculations based on a full-dimensional analytical potential energy surface, PES-1997, developed in our research group.³ This PES is the only analytical surface proposed for this reaction and is basically a valence-bond molecular-mechanics (VB-MM) surface with adjustable parameters. It presents high exothermicity, $-25.80 \text{ kcal mol}^{-1}$, in excellent agreement with recent high-level ab initio calculations,⁴ $-25.77 \text{ kcal mol}^{-1}$. In addition, it presents an $\text{F}\cdots\text{H}_3\text{N}$ van der Waals complex in the entry channel (face configuration: the fluorine atom approaches the N atom of NH_3 , with the three H atoms on the same side, $\text{F}\cdots\text{H}_3\text{N}$), stabilized by $6.11 \text{ kcal mol}^{-1}$ with respect to the reactants, and an $\text{H}_2\text{N}\cdots\text{HF}$ hydrogen bond complex in the exit channel, stabilized by $6.25 \text{ kcal mol}^{-1}$ with respect to the products, reproducing qualitatively the tendency found using high-level ab initio calculations,⁴ 12.28 and $9.94 \text{ kcal mol}^{-1}$, respectively, given the semiempirical character of the PES and that at that time (1997) these complexes were not determined and therefore not included in the fitting procedure.³ In that study⁶ we found that recent crossed-beam experiments reported by Xiao et al.⁴ at $4.5 \text{ kcal mol}^{-1}$ are reproduced, providing confidence to the PES-1997 surface.

In the present work, thermal rate coefficients were calculated using two dynamical approaches, ring polymer molecular dynamics (RPMD) and QCT, both based on the analytical PES-1997 surface, and compared with available experimental values. Given that the PES-1997 presents a complex in the entry channel, this calculation represents an excellent opportunity to test Persky's hypothesis that the inverse temperature dependence of the rate coefficients is due to the presence of this complex.

2. METHODS AND COMPUTATIONAL DETAILS

2.1. Potential Energy Surface. The analytical PES-1997 function was developed in our previous study³ and therefore will be only briefly described here. It is basically a valence bond-molecular mechanics (VB-MM) surface, given by the sum of three terms: a stretching potential, V_{stretch} , a harmonic bending term, V_{harm} , and an anharmonic out-of-plane potential, V_{op}

$$V = V_{\text{stretch}} + V_{\text{harm}} + V_{\text{op}} \quad (1)$$

and it was designed to describe exclusively the hydrogen abstraction reaction.

The stretching potential is the sum of three London–Eyring–Polanyi (LEP) terms, each one corresponding to a permutation of the three ammonia hydrogens

$$V_{\text{stretch}} = \sum_{i=1}^3 V_3(R_{\text{NH}_i}, R_{\text{NF}}, R_{\text{H}_i\text{F}}) \quad (2)$$

where R is the distance between the two subscript atoms, and H_i stands for one of the three ammonia hydrogens. Note that 14 fitting parameters are required to describe this stretching potential.

The V_{harm} term is the sum of three harmonic terms, one for each bond angle in ammonia

$$V_{\text{harm}} = \frac{1}{2} \sum_{i=1}^2 \sum_{j=i+1}^3 k_{ij}^0 k_i (\theta_{ij} - \theta_{ij}^0)^2 \quad (3)$$

where k_{ij}^0 and k_i are force constants, and θ_{ij}^0 are the reference angles. The k_{ij}^0 force constants are allowed to evolve from their

value in ammonia, k^{NH_3} , to their value in the amidogen radical, k^{NH_2} , corresponding to two parameters of the fit, by means of switching functions. In total, 16 parameters need to be fitted for the calibration of the V_{harm} potential.

The V_{op} potential is a quadratic-quartic term whose aim is to correctly describe the out-of-plane motion of ammonia³

$$V_{\text{op}} = \sum_{i=1}^3 f_{\Delta_i} \sum_{j=1, j \neq i}^3 (\Delta_{ij})^2 + \sum_{i=1}^3 h_{\Delta_i} \sum_{j=1, j \neq i}^3 (\Delta_{ij})^4 \quad (4)$$

The force constants, f_{Δ_i} and h_{Δ_i} , have been incorporated into a switching function, which is such that V_{op} vanishes at the amidogen radical limit. Δ_{ij} is the angle that measures the deviation from the reference angle

$$\Delta_{ij} = \arccos \left(\vec{N}_i \frac{\vec{r}_j}{\|\vec{r}_j\|} \right) - \theta_{ij}^0 \quad (5)$$

where \vec{N}_i is a unit vector normal to the plane defined by the three hydrogen atoms of the ammonia and θ_{ij}^0 is the reference angle. The vector \vec{N}_i is given by

$$\vec{N}_i = \frac{(\vec{r}_k - \vec{r}_j) \times (\vec{r}_l - \vec{r}_j)}{\|(\vec{r}_k - \vec{r}_j) \times (\vec{r}_l - \vec{r}_j)\|} \quad i = 1, 2, 3 \quad (6)$$

where \vec{r}_p , \vec{r}_k , and \vec{r}_l are vectors going from the nitrogen atom to the j , k , and l hydrogen atoms, respectively, in ammonia. To correctly calculate Δ_{ij} , the motion from j to l has to be clockwise. In total, 4 parameters need to be fitted for the calibration of the V_{op} potential.

Note that in the original expression, the V_{op} term was added to obtain a correct description of the umbrella mode of ammonia. Although recently Yang and Corchado¹⁹ noted that this term yields nonphysical behavior along the ammonia inversion path (which was not taken into account originally), this problem is of no importance in the present case because only the hydrogen abstraction reaction is being considered.

The PES-1997 is symmetric with respect to the permutation of the three equivalent ammonia hydrogens, a feature that is especially important in dynamics calculations. It depends on 34 parameters: 14 for the stretching, 16 for the harmonic term, and 4 for the out-of-plane potential. These 34 parameters endow the PES with great flexibility, while keeping the VB/MM functional form physically intuitive.

Once the functional form was available, the 34 parameters describing the PES-1997 were fitted by using as input information a combination of theoretical and experimental data (see original paper for more details). In this sense, therefore, the surface is semiempirical.

2.2. Kinetics Calculations. The thermal rate coefficients calculations of the title reaction were performed based on the PES-1997 surface using two different approaches.

Approach 1: Ring Polymer Molecular Dynamics (RPMD) Calculations.^{20,21} The RPMD method exploits the isomorphism between the statistical properties of the quantum system and those of a classical fictitious ring polymer consisting of many copies of the original system connected by harmonic springs.²² This isomorphism enables the automatic inclusion of quantum effects via classical molecular dynamics simulations in an extended phase space. Application of RPMD to gas phase bimolecular chemical reactions^{23–32} has demonstrated that it provides systematic and consistent performance across a wide

range of system dimensionalities. In all systems considered so far, the RPMD rate coefficient captures almost perfectly the ZPE effect and is usually within a factor of 2–3 of accurate results at very low temperatures in the deep quantum tunnelling regime when compared to rigorous quantum mechanical results available for these systems. Most chemical reactions can be studied using RPMD with only about 1–2 orders of magnitude higher computational costs than conventional QCT calculations.

The RPMD calculations were carried out using the RPMDrate code developed by one of us;²⁹ the working equations of the RPMD rate theory can be found in refs 24 and 27. The title system has one bond that forms and breaks in the reaction and three equivalent product arrangement channels. The transition state dividing surface was placed at an intermediate saddle point between the two complexes in the entry and exit channels of the PES-1997 and was defined in the same way as previously for thermally activated reaction in terms of the bond-breaking and bond-forming distances as discussed in ref 29. Initial distance between the reactants was set to $20a_0$. Number of beads of the ring polymer was set to 128 for all temperatures considered. The transmission coefficients were computed at various positions of the reaction coordinate ξ in the interval between 0.4 and 0.7, which correspond to the maximum values of the potential of mean force that occur before the reactant intermediate complex (see Figure 1). We

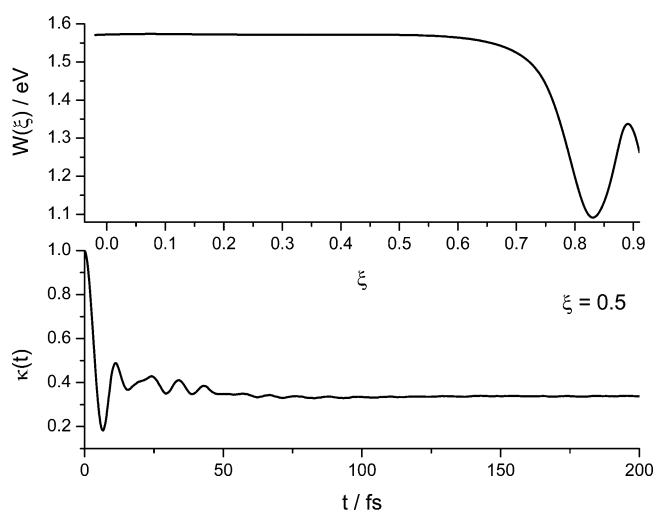


Figure 1. RPMD potential of mean force (upper panel) and RPMD transmission coefficient calculated at $\xi = 0.5$ (lower panel) for the F + NH_3 reaction at 298 K. Note that these profiles are practically the same for the other two temperatures of interest (276 and 327 K).

verified that shifting the position of the starting point for the transmission coefficient calculations did not change the final RPMD rate coefficient. For these calculations, the child trajectories were propagated for 0.3 ps where the transmission coefficients reached plateau values. All other parameters can be

found in Table 1 of the RPMDrate manuscript.²⁹ Finally, we included the $^2\text{P}_{1/2}$ excited state of fluorine (with an excitation function of $\varepsilon = 404 \text{ cm}^{-1}$)³³ in the reactant electronic partition function

$$\frac{Q_e^{\text{TS}}}{Q_e^{\text{reactants}}} = \frac{2}{4 + 2 \exp(-\varepsilon/k_b T)} \quad (7)$$

It is interesting to note that the present study is one of the first applications of this method to polyatomic barrierless reactions (see also ref 31).

Approach 2: Quasi-Classical Trajectory (QCT) Calculations. Quasi-classical trajectory calculations were carried out using the VENUS96 code.³⁴ The accuracy of the trajectories was checked by the conservation of the total energy and the total angular momentum. Batches of 50 000 trajectories were run with different collision energies ranging from 0.1 to 4.0 kcal mol^{-1} ; thermal distributions of rotational and vibrational energies at 276, 298, and 327 K were used as initial conditions for the reactants, with an integration step of 0.01 fs. The maximum impact parameter, b_{max} , was set from 6.2 to 4.0 Å in the energy range considered, after testing for a wide set of initial conditions and checking that the final results were not influenced by this parameter. For each energy, the maximum value of the impact parameter, b_{max} , was determined by first calculating batches of 10 000 trajectories at fixed values of the impact parameter, b , systematically increasing the value of b until no reactive trajectories were obtained.

The QCT reaction cross-section is defined as

$$\sigma_r = \pi b_{\text{max}}^2 (N_r/N_T) \quad (8)$$

where N_r and N_T are the number of reactive and total trajectories, respectively, and its ratio is the reaction probability. A large number of trajectories ($N_T = 50000$) was used to ensure converged sampling with respect to the impact parameter and rovibrational states so that the obtained results do not depend on the averaging method.

One of the major difficulties with the quasi-classical simulations is the question of how to handle the ZPE correction. Various strategies have been proposed to take into account this quantum-mechanical effect (see refs 35–43 and references therein), but no completely satisfactory approach exists. Here we employed a pragmatic solution, the so-called passive method,⁴⁰ which consists of running the trajectories with no quantum constraint and subsequent analysis and discarding those that are not allowed in the quantum mechanical world, even though this method is known to perturb the statistics and can therefore lead to uncertainties in the dynamics study.⁴⁴ In particular, in N_r we discard all the reactive trajectories for which either of the products has a vibrational energy lower than its harmonic ZPE. We call this histogram binning with double ZPE correction (HB-DZPE). However, this way of removing trajectories from the N_r count without taking into account the behavior of the total ensemble

Table 1. Thermal Forward Rate Coefficients ($\text{cm}^3 \text{ molecule}^{-1} \text{ s}^{-1}$) for the F + NH_3 Reaction

T (K)	RPMD/PES-1997	QCT/PES-1997	exptl ^a	exptl ^b
276	4.63×10^{-10}	5.48×10^{-10}	3.60×10^{-10}	2.34×10^{-11}
298	4.40×10^{-10}	5.63×10^{-10}	1.00×10^{-10}	2.85×10^{-11}
327	4.80×10^{-10}	5.72×10^{-10}	9.00×10^{-11}	3.37×10^{-11}

^aRef 15. ^bRef 18.

of trajectories can lead to erroneous results because as mentioned above it modifies the statistics.⁴⁴ So, the total number of trajectories, N_T in eq 8, is replaced by the total number of trajectories minus the number of reactive trajectories whose final vibrational energy is below the ZPE of the two products and minus the number of nonreactive trajectories whose final vibrational energy is below the ZPE of the NH_3 reactant.

Finally, rate coefficients were computed by numerical integration of the cross-sections

$$k(T) = \left(\frac{2}{k_b T} \right)^{3/2} \left(\frac{1}{\pi \mu} \right)^{1/2} \int E \sigma_r(E) \exp(-E/k_b T) dE \quad (9)$$

where E is the collision energy and μ is the reduced mass of the reaction. Note that for this barrierless reaction the tunnelling effect is negligible, and therefore, the use of this quasi-classical approach seemed to be reasonable.

3. RESULTS AND DISCUSSION

In the hydrogen abstraction mechanism, the F atom approaches the NH_3 molecule through a very stabilized complex in the entry channel, and it is a barrierless process. In this section we begin analyzing the rate coefficients calculations using the RPMD/PES-1997 approach. Figure 1 shows the ring polymer potential of mean force (PMF) (upper panel) and the transmission coefficient (lower panel) calculated at temperature 298 K. As expected, the PMF profile demonstrates the presence of the complex in the reactant channel. The transmission coefficient exhibit several oscillations, and the plateau time of 0.3 ps is higher than observed previously for thermally activated reactions (with barrier).^{23–32} Another distinctive feature of the present RPMD calculations for barrierless reaction is the fact that these profiles practically do not change for the other two temperatures of interest (276 and 327 K). Table 1 lists the forward rate coefficients in the temperature range 276–327 K, and experimental values^{15,18} are included for comparison as well. Figure 2 shows these results. The small difference between the RPMD rate coefficients at different temperatures is, in fact, within the convergence limits of the present calculations.

The rate coefficients calculated using the QCT/PES-1997 approach also appear in Table 1 and Figure 2. Of particular note is that both QCT and RPMD results obtained using the same PES-1997 do not differ significantly, confirming the accuracy of our approach for the ZPE correction of the QCT calculations and that tunnelling, which is captured only by the RPMD method, does not contribute to the title barrierless reaction. Finally, as was expected, the HB-DZPE correction to the QCT calculations diminishes the rate coefficients, although they also present a variation independent of temperature.

Quantitatively, the theoretical results are 1 order of magnitude larger than those of Walther–Wagner's¹⁸ and are in reasonable agreement with Persky's values¹⁵ at the lowest temperature (276 K), especially the RPMD approach. In addition, they show that the rate coefficients are practically independent of temperature. This behavior agrees with the Walther–Wagner's experiments,¹⁸ but disagrees with Persky's more recent experiment,¹⁵ which presents a strong variation in this small temperature range. Given that the PES-1997 surface presents a well in the entry channel and that the theoretical study does not report sudden changes, this can not be the cause of the variation with the temperature suggested by Persky.

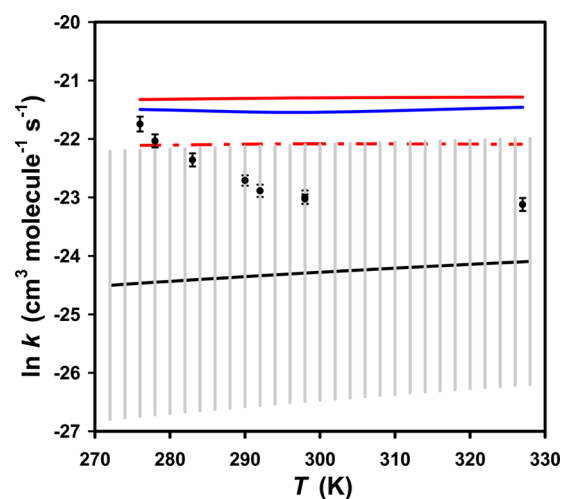


Figure 2. Plot of $\ln k$ ($\text{cm}^3 \text{ molecule}^{-1} \text{ s}^{-1}$) against the temperature (K) in the range 276–327 K. Solid black circles, Persky's experimental values; black line, Walther and Wagner's experimental values (the uncertainty region is shown shaded); blue line, RPMD calculations on PES-1997; solid red line, QCT calculations on PES-1997; dashed red line, QCT calculations using the HB-DZPE constraint.

However, in an attempt to understand this difference with Persky's experiment, we have considered the following two issues:

- Comparison with similar fast reactions. We analyzed the recent literature on similar very fast reactions and found no behavior like that observed in Persky's experiment in such a small temperature range. For instance, Bahng and Macdonald⁴⁵ determined the rate coefficients for the $\text{OH} + \text{OH}$ reaction over the temperature range 203–373 K, which were practically independent of the temperature, $2.7\text{--}2.2 \times 10^{-12} \text{ cm}^3 \text{ molecule}^{-1} \text{ s}^{-1}$. Jasper et al.⁴⁶ found that the capture coefficient for the $\text{CH}_3 + \text{OH}$ reaction was almost independent of the temperature, suggesting that the discrepancies with experiment is a result of falloff in the experimental results. For the ClO self-reaction, Ferracci and Rowley⁴⁷ found that the temperature dependence obtained over the temperature range 298–323 K was considerably less pronounced than that previously reported. Finally, the kinetics of the $\text{OH} + \text{CO}$ reaction has been extensively studied^{48–52} revealing that the rate coefficient remains almost invariant at low temperature, only increasing sharply with temperature above 500 K. Note, however, that the fact that Persky's temperature dependence has not been observed in other systems does not in any way suggest the experiment is incorrect.
- Effect of the secondary reaction in the title reaction. As was indicated in the Introduction, the title reaction is very fast, followed by the even faster secondary reaction, $\text{F} + \text{NH}_2 \rightarrow \text{HF} + \text{NH}$. We propose the following hypothesis: could the temperature dependence be due to the presence of fast secondary reactions in the experiment?

To analyze this supposition, we considered two similar fast hydrogen abstraction reactions followed by very fast secondary reactions, $\text{OH} + \text{NH}_3/\text{NH}_2$ and $\text{O}(^3\text{P}) + \text{NH}_3/\text{NH}_2$, whose experimental rate coefficients are well-known^{53–55} (Table 2). In both reactions, the secondary reactions are faster than the

Table 2. Experimental Rate Coefficients ($\text{cm}^3 \text{ molecule}^{-1} \text{ s}^{-1}$) for the $\text{OH} + \text{NH}_3/\text{NH}_2$ and $\text{O}(^3\text{P}) + \text{NH}_3/\text{NH}_2$ Reactions and Relative Increase for Each Reaction

T (K)	$\text{OH} + \text{NH}_2^a$	$\text{OH} + \text{NH}_3^b$	quotient ^c	relative quotient ^d
250	1.48×10^{-12}	0.865×10^{-13}	17.11	2.80
275	1.57	1.21	12.97	2.12
300	1.67	1.60	10.44	1.71
325	1.77	2.03	8.72	1.43
350	1.88	2.49	7.55	1.24
375	2.00	2.97	6.73	1.10
400	2.12	3.47	6.11	1.00
T (K)	$\text{O}(^3\text{P}) + \text{NH}_2^a$	$\text{O}(^3\text{P}) + \text{NH}_3^b$	quotient	relative quotient
250	1.19×10^{-11}			
275	1.18			
300	1.18	0.469×10^{-16}	2.51E05	16.00
325	1.18	1.09	1.08	6.88
350	1.19	2.26	0.526	3.35
375	1.19	4.30	0.276	1.76
400	1.20	7.62	0.157	1.0

^aRef 53. ^bRef 54. ^cQuotient: $k(\text{OH} + \text{NH}_2)/k(\text{OH} + \text{NH}_3)$. ^dRelative quotient: $k(T)/k(400 \text{ K})$, where the value at 400 K takes the unity.

primary ones, by factors of 10.44 and 2.51×10^5 , respectively, at 300 K. However, more interesting is the variation of this increase with temperature. So, taking as a reference the highest temperature analyzed, 400 K (value unity), in the $\text{OH} + \text{NH}_3/\text{NH}_2$ reactions, the secondary reaction is ~ 3 times faster at 250 K; while in the $\text{O}(^3\text{P}) + \text{NH}_3/\text{NH}_2$ reactions, the secondary reaction is ~ 16 times faster at 300 K. In sum, the lower the temperature, the faster the secondary reaction. Assuming similar behavior for the title reaction $\text{F} + \text{NH}_3/\text{NH}_2$, if in the experiment the secondary reaction $\text{F} + \text{NH}_2 \rightarrow \text{HF} + \text{NH}$ occurs (in whole or in part), its faster rate coefficients could contaminate the primary one, more strongly as the temperature decreases.

Therefore, further studies should be carried out to solve the disagreement between theory and experiment in the title reaction. In this context new experiments on the system over a larger range of temperatures would be of great help. From the theory point of view a possible further step in this work would be to explicitly evaluate the spin–orbit coupling along the reaction path and to construct more accurate global analytical PES for further dynamics studies with such advanced techniques as RPMD.

4. CONCLUSIONS

In this work we have investigated the gas-phase reaction $\text{F} + \text{NH}_3 \rightarrow \text{HF} + \text{NH}_2$ using an analytical full-dimensional potential energy surface, PES-1997, and two dynamical approaches: RPMD and QCT. We found that when the fluorine atom approaches to NH_3 the reaction evolves without barrier, with stabilized intermediate complexes in the entrance and exit channels.

Both RPMD and QCT thermal rate coefficients present a behavior that is practically independent of temperature. In the common temperate range, 276–327 K, this behavior agrees with the Walther–Wagner's experimental measures, although quantitatively our results are higher by 1 order of magnitude. In contrast, our results show a reasonable agreement with Persky's more recent values¹⁵ at the lowest temperature (276 K), especially the RPMD method, which seems to suggest that Walther–Wagner's older values could be underestimated.

However, the theoretical values disagree with the variation with temperature reported by Persky, which show a sudden change of behavior in this very small temperature range, which to our knowledge, have never been reported for similar fast reactions. To explain this behavior, Persky suggested an intermediate complex in the entry channel. The PES-1997 shows a van der Waals complex in the entry channel, but the theoretical results obtained in the present work show that it is not associated with any sudden changes in the kinetics results. Therefore, further theoretical and experimental studies are needed to understand this discrepancy.

AUTHOR INFORMATION

Corresponding Author

*(J.E.-G.) E-mail: joaquin@unex.es.

Notes

The authors declare no competing financial interest.

ACKNOWLEDGMENTS

This work was partially supported by Gobierno de Extremadura, Spain, and FEDER (Project No. IB10001). Y.V.S. acknowledges the support of a Combustion Energy Research Fellowship through the Combustion Energy Frontier Research Center, an Energy Frontier Research Center funded by the U.S. Department of Energy, Office of Basic Energy Sciences under Award Number DE-SC0001198. A.F.-R. thanks Xunta de Galicia through Grant No. 2012/314 para a consolidación e a estruturação de unidades de investigación competitivas do Sistema Universitario de Galicia, 2012.

REFERENCES

- (1) Goddard, J. D.; Donaldson, D. J.; Sloan, J. J. Hydrogen Bonded Complexes and the HF Vibrational Energy Distributions from the Reaction of F-Atoms with NH_2 and NH_3 . *Chem. Phys.* **1987**, *114*, 321–329.
- (2) Leroy, G.; Sana, M.; Tinant, A. Etude theorique des reactions d'abstractions d'hydrogene $\text{RH} + \text{X} = \text{R} + \text{HX}$ avec $\text{R} = \text{H}$, CH_3 , NH_2 , OH et F . *Can. J. Chem.* **1985**, *63*, 1447–1456.
- (3) Espinosa-Garcia, J.; Corchado, J. C. Analytical Surface for the Reaction with No Saddle-Point $\text{NH}_3 + \text{F} \rightarrow \text{NH}_2 + \text{FH}$. Application of Variational Transition State Theory. *J. Phys. Chem. A* **1997**, *101*, 7336–7344.
- (4) Xiao, G.; Shen, G.; Wang, X.; Fan, H.; Yang, X. Crossed Beams Study on the Dynamics of the F-Atom Reaction with Ammonia. *J. Phys. Chem. A* **2010**, *114*, 4520–4523.
- (5) Feng, H.; Sun, W.; Xie, Y.; Schaefer, H. F. Is There an Entrance Complex for the $\text{F} + \text{NH}_3$ Reaction? *Chem.—Asian J.* **2011**, *6*, 3152–3156.
- (6) Espinosa-Garcia, J.; Monge-Palacios, M. Theoretical Study of the $\text{F} + \text{NH}_3$ and $\text{F} + \text{ND}_3$ Reactions: Mechanism and Comparison with Experiment. *J. Phys. Chem. A* **2011**, *115*, 13759–13763.
- (7) Duewer, W. H.; Setser, D. W. Infrared Chemiluminescence and Energy Partitioning from Reactions of Fluorine Atoms with Hydrides of Carbon, Silicon, Oxygen, Sulfur, Nitrogen, and Phosphorus. *J. Chem. Phys.* **1973**, *58*, 2310–2320.
- (8) Douglas, D. J.; Sloan, J. J. The Dynamics of the Reactions of Fluorine Atoms with Ammonia and Hydrazine. *Chem. Phys.* **1980**, *46*, 307–312.
- (9) Sloan, J. J.; Watson, D. G.; Williamson, J. The Detailed Isotope Effect in the $\text{F} + \text{NH}_3$ and $\text{F} + \text{ND}_3$ Reactions. *Chem. Phys. Lett.* **1980**, *74*, 481–485.
- (10) Manocha, D. S.; Setser, D. W.; Wickramaaratchi, M. Vibrational Energy Disposal in Reactions of Fluorine Atoms with Hydrides of Groups III, IV and V. *Chem. Phys.* **1983**, *76*, 129–146.

- (11) Donaldson, D. J.; Parsons, J.; Solan, J. J.; Stolow, A. Vibrational Energy Partitioning in the Reaction of F Atoms with NH_3 and ND_3 . *Chem. Phys.* **1984**, *85*, 47–62.
- (12) Donaldson, D. J.; Sloan, J. J.; Goddard, J. D. Energy Partitioning in the Reaction of F-Atoms with NH_2 Radicals. *J. Chem. Phys.* **1985**, *82*, 4524–4536.
- (13) Wategaonkar, S.; Setser, D. W. Vibrational Energy Disposal in the Reactions of F Atoms with NH_3 , ND_3 , N_2H_4 , and CH_3ND_2 . *J. Chem. Phys.* **1987**, *86*, 4477–4487.
- (14) Sloan, J. J. On the Dynamics of Abstraction, Insertion, and Addition–Elimination Reactions in the Gas Phase. *J. Phys. Chem.* **1988**, *92*, 18–27.
- (15) Persky, A. The Rate Constant of the $\text{F} + \text{NH}_3$ Reaction: Inverse Temperature Dependence. *Chem. Phys. Lett.* **2007**, *439*, 3–7.
- (16) Misochko, E. Y.; Goldschleger, I. U.; Akimov, A. V.; Wight, C. A. Infrared and EPR Spectroscopic Study of Open-Shell Reactive Intermediates: $\text{F} + \text{NH}_3$ in Solid Argon. *Low Temp. Phys.* **2000**, *26*, 727–735.
- (17) Goldschleger, I. U.; Akimov, A. V.; Misochko, E. Y. EPR Spectroscopy of the Radical-Molecular Complex $\text{NH}_2\text{-HF}$ Formed in Low Temperature Chemical Reaction of Fluorine Atoms with NH_3 Molecules Trapped in Solid Argon. *J. Mol. Struct.* **2000**, *519*, 191–197.
- (18) Walther, C. D.; Wagner, H. G. Über die Reaktionen von F-Atomen mit H_2O , H_2O_2 und NH_3 . *Ber. Bunsenges. Phys. Chem.* **1983**, *87*, 403–409.
- (19) Yang, M.; Corchado, J. C. Seven-Dimensional Quantum Dynamics Study of the $\text{H} + \text{NH}_3 \rightarrow \text{H}_2 + \text{NH}_2$ Reaction. *J. Chem. Phys.* **2007**, *126*, 214312.
- (20) Craig, I. R.; Manolopoulos, D. E. Chemical Reaction Rates from Ring Polymer Molecular Dynamics. *J. Chem. Phys.* **2005**, *122*, 084106; A Refined Ring Polymer Molecular Dynamics Theory of Chemical Reaction Rates. *J. Chem. Phys.* **2005**, *123*, 034102.
- (21) Suleimanov, Y. V. Surface Diffusion of Hydrogen on $\text{Ni}(100)$ from Ring Polymer Molecular Dynamics. *J. Phys. Chem. C* **2012**, *116*, 11141–11153.
- (22) Chandler, D.; Wolynes, P. G. Exploiting the Isomorphism between Quantum Theory and Classical Statistical Mechanics of Polyatomic Fluids. *J. Chem. Phys.* **1981**, *74*, 4078–4095.
- (23) Collepardo-Guevara, R.; Suleimanov, Y. V.; Manolopoulos, D. E. Bimolecular Reaction Rates from Ring Polymer Molecular Dynamics. *J. Chem. Phys.* **2009**, *130*, 174713; Erratum. *J. Chem. Phys.* **2010**, *133*, 049902.
- (24) Pérez de Tudela, R.; Aoiz, F. J.; Suleimanov, Y. V.; Manolopoulos, D. E. Chemical Reaction Rates from Ring Polymer Molecular Dynamics: Zero Point Energy Conservation in $\text{Mu} + \text{H}_2 \rightarrow \text{MuH} + \text{H}$. *J. Phys. Chem. Lett.* **2012**, *3*, 493–497.
- (25) Suleimanov, Y. V.; Pérez de Tudela, R.; Jambrina, P. G.; Castillo, J. F.; Sáez-Rábanos, V.; Manolopoulos, D. E.; Aoiz, F. J. A Ring Polymer Molecular Dynamics Study of the Isotopologues of the $\text{H} + \text{H}_2$ Reaction. *Phys. Chem. Chem. Phys.* **2013**, *15*, 3655–3665.
- (26) Suleimanov, Y. V.; Collepardo-Guevara, R.; Manolopoulos, D. E. Bimolecular Reaction Rates from Ring Polymer Molecular Dynamics: Application to $\text{H} + \text{CH}_4 \rightarrow \text{H}_2 + \text{CH}_3$. *J. Chem. Phys.* **2011**, *134*, 044131.
- (27) Li, Y.; Suleymanov, Y. V.; Yang, M.-H.; Green, W. H.; Guo, H. Rate Coefficients and Kinetic Isotope Effects of the $\text{X} + \text{CH}_4 \rightarrow \text{CH}_3 + \text{HX}$ ($\text{X} = \text{H}, \text{D}, \text{Mu}$) Reactions from Ring Polymer Molecular Dynamics. *J. Chem. Phys.* **2013**, *138*, 094307.
- (28) Li, Y.; Suleymanov, Y. V.; Yang, M. H.; Green, W. H.; Guo, H. Ring Polymer Molecular Dynamics Calculations of Thermal Rate Constants for the $\text{O}(^3\text{P}) + \text{CH}_4 \rightarrow \text{OH} + \text{CH}_3$ Reaction: Contributions of Quantum Effects. *J. Phys. Chem. Lett.* **2013**, *4*, 48–52.
- (29) Suleymanov, Y. V.; Allen, J. W.; Green, W. H. RPMD rate: Bimolecular chemical reaction rates from ring polymer molecular dynamics. *Comput. Phys. Commun.* **2013**, *184*, 833–840.
- (30) Allen, J. W.; Green, W. H.; Li, Y.; Guo, H.; Suleymanov, Y. V. Communication: Full Dimensional Quantum Rate Coefficients and Kinetic Isotope Effects from Ring Polymer Molecular Dynamics for a Seven-Atom Reaction $\text{OH} + \text{CH}_4 \rightarrow \text{CH}_3 + \text{H}_2\text{O}$. *J. Chem. Phys.* **2013**, *138*, 221103.
- (31) Perez de Tudela, R.; Suleymanov, Y. V.; Menendez, M.; Castillo, F. J.; Manolopoulos, D. E.; Aoiz, F. J. In preparation.
- (32) Li, Y.; Suleymanov, Y. V.; Green, W. H.; Guo, H. In preparation.
- (33) Chase, M. W.; Davis, C. A.; Downey, J. R.; Frurip, D. J.; McDonald, R. A.; Syverud, A. N. JANAF Thermochemical Tables. *J. Phys. Chem. Ref. Data Suppl.* **1985**, *14*.
- (34) Hase, W. L.; Duchovic, R. J.; Hu, X.; Komornicki, A.; Lim, K. F.; Lu, D. H.; Peslherbe, G. H.; Swamy, K. N.; Vande Linde, S. R.; Varandas, A. J. C.; et al. VENUS96: A General Chemical Dynamics Computer Program. *QCPE Bull.* **1996**, *16*, 43.
- (35) Wu, S. F.; Marcus, R. A. Analytical Mechanics of Chemical Reactions. V. Application to the Linear Reactive $\text{H} + \text{H}_2$ Systems. *J. Chem. Phys.* **1970**, *53*, 4026–4034.
- (36) Bowman, J. M.; Kuppermann, A. Comparison of Semiclassical, Quasiclassical, and Exact Quantum Transition Probabilities for the Collinear $\text{H} + \text{H}_2$ Exchange Reaction. *J. Chem. Phys.* **1973**, *59*, 6524–6534.
- (37) Truhlar, D. G. Accuracy of Trajectory Calculations and Transition State Theory for Thermal Rate Constants of Atom Transfer Reactions. *J. Phys. Chem.* **1979**, *83*, 188–199.
- (38) Schatz, G. C. The Origin of Cross Section Thresholds in $\text{H} + \text{H}_2$: Why Quantum Dynamics Appears to Be More Vibrationally Adiabatic than Classical Dynamics. *J. Chem. Phys.* **1983**, *79*, 5386–5391.
- (39) Lu, D. H.; Hase, W. L. Classical Mechanics of Intramolecular Vibrational Energy Flow in Benzene. IV. Models with Reduced Dimensionality. *J. Chem. Phys.* **1988**, *89*, 6723–6735.
- (40) Varandas, A. J. C. A Novel Non-Active Model to Account for the Leak of Zero-Point Energy in Trajectory Calculations. Application to $\text{H} + \text{O}_2$ Reaction near Threshold. *Chem. Phys. Lett.* **1994**, *225*, 18–27.
- (41) Bonnet, L.; Rayez, J. C. Quasiclassical Trajectory Method for Molecular Scattering Processes: Necessity of a Weighted Binning Approach. *Chem. Phys. Lett.* **1997**, *277*, 183–190.
- (42) Marques, J. M. C.; Martinez-Núñez, E.; Fernandez-Ramos, A.; Vazquez, S. Trajectory Dynamics Study of the $\text{Ar} + \text{CH}_4$ Dissociation Reaction at High Temperatures: the Importance of Zero-Point-Energy Effects. *J. Phys. Chem.* **2005**, *109*, 5415–5423.
- (43) Duchovic, R. J.; Parker, M. A. A Quasiclassical Trajectory Study of the Reaction $\text{H} + \text{O}_2 \rightleftharpoons \text{OH} + \text{O}$ with the O_2 Reagent Vibrationally Excited. *J. Phys. Chem.* **2005**, *109*, 5883–5896.
- (44) Guo, Y.; Thomson, D. L.; Sewell, T. D. Analysis of the Zero-Point Energy Problem in Classical Trajectory Simulations. *J. Chem. Phys.* **1996**, *104*, 576–582.
- (45) Bahng, M.-K.; Macdonald, R. G. Determination of the Rate Constant for the $\text{OH}(X^2\Pi) + \text{OH}(X^2\Pi) \rightarrow \text{O}(^3\text{P}) + \text{H}_2\text{O}$ Reaction over the Temperature Range 293–373 K. *J. Phys. Chem. A* **2007**, *111*, 3850–3861.
- (46) Jasper, A. W.; Klippenstein, S. J.; Harding, L. B.; Ruscic, B. Kinetics of the Reaction of Methyl Radical with Hydroxyl Radical and Methanol Decomposition. *J. Phys. Chem. A* **2007**, *111*, 3932–3950.
- (47) Ferracci, V.; Rowley, D. M. The Temperature Dependence of the Bimolecular Channels of the $\text{ClO} + \text{ClO}$ Reaction over the Range $T = 298\text{--}323\text{ K}$. *Int. J. Chem. Kinet.* **2012**, *44*, 386–397.
- (48) Smith, I. W. M.; Zellner, R. Rate Measurements of Reactions of OH by Resonance Absorption. Part 2. Reactions of OH with CO, C_2H_4 and C_2H_2 . *J. Chem. Soc., Faraday Trans. 2* **1973**, *69*, 1617–1627.
- (49) Ravishankara, A. R.; Thompson, R. L. Kinetic Study of the Reaction of OH with CO from 250 to 1040 K. *Chem. Phys. Lett.* **1983**, *99*, 377–381.
- (50) Frost, M. J.; Sharkey, P.; Smith, I. W. M. Reaction between Hydroxyl (Deuteroxyl) Radicals and Carbon Monoxide at Temperatures down to 80 K: Experiment and Theory. *J. Phys. Chem.* **1993**, *97*, 12254–12259.
- (51) Fulle, D.; Hamann, H. F.; Hippler, H.; Troe, J. High Pressure Range of Addition Reactions of HO. II. Temperature and Pressure

Dependence of the Reaction $\text{HO} + \text{CO} = \text{HOCO} \rightarrow \text{H} + \text{CO}_2$. *J. Chem. Phys.* **1996**, *105*, 983–1000.

(52) Golden, D. M.; Smith, G. P.; McEwen, A. B.; Yu, C.-L.; Eiteneer, B.; Frenklach, M.; Vaghjiani, G. L.; Ravishankara, A. R.; Tully, F. P. $\text{OH(OD)} + \text{CO}$: Measurements and an Optimized RRKM Fit. *J. Phys. Chem. A* **1998**, *102*, 8598–8606.

(53) Cohen, N.; Westberg, K. R. Chemical Kinetic Data Sheets for High-Temperature Reactions. Part II. *J. Phys. Chem. Ref. Data* **1991**, *20*, 1211–1312.

(54) Atkinson, R.; Baulch, D. L.; Cox, R. A.; Crowley, J. N.; Hampson, R. F.; Hynes, R. G.; Jenkin, M. E.; Rossi, M. J.; Troe, J. Evaluated Kinetic and Photochemical Data for Atmospheric Chemistry: Volume I, Gas Phase Reactions of O_x , HO_x , NO_x and SO_x Species. *Atmos. Chem. Phys.* **2004**, *4*, 1461–1738.

(55) Bozzelli, J. W.; Dean, A. M. Energized Complex Quantum Rice–Ramsperger–Kassel Analysis on Reactions of Amidogen with Hydroperoxo, Oxygen and Oxygen Atoms. *J. Phys. Chem.* **1989**, *93*, 1058–1065.